S1 Target VOC signals and detection limits

Table S1 summarizes the target VOC signals used in the 1900D PTR-ToF-MS analysis and the detection limits for the 10 s averaged data. C_8 aromatics are reported as the unresolved sum of xylenes and ethylbenzene, and m/z 73.065 is reported as a methyl ethyl ketone (MEK)-equivalent signal because possible isobaric oxygenated VOC contributions cannot be fully excluded. Trimethylbenzenes were not directly calibrated; their sensitivity was estimated from the mass-transmission relationship.

Detection limits (DLs) for the 10 s averaged data were determined from the variability of zero-air measurements after applying the same 10 s rolling mean used for the ambient data. DLs were defined as 3.3 times the standard deviation of the blank signal ($3.3\sigma_{blank}$).

Table S1: Analytical information for target VOC signals quantified by the PTR-ToF-MS aboard the 1900D during the ASIA-AQ campaign. Detection limits refer to the 10 s averaged data.

Substance / signal	Abbrev.	Molecular formula	Protonated mass (m/z)	Boiling point (°C)	Proton affinity (kJ mol^{-1})	10 s DL (ppbv)
Acetonitrile	AN	C_2H_3N	42.034	81.3–82.1	779.2	0.05
Acetone	ACT	C_3H_6O	59.049	56.1	812	0.06
MEK-equivalent signal	MEK	C_4H_8O	73.065	79.6	827.3	0.10
Benzene	BZ	C_6H_6	79.054	80.1	750.4	0.03
Toluene	TOL	C_7H_8	93.070	111	784.3	0.06
C_8 aromatics (xylenes + ethylbenzene)	C_8	C_8H_{10}	107.086	138.5[a]	796[a]	0.02
Trimethylbenzenes	TMB	C_9H_{12}	121.101	169–171	798.3[b]	—

[a] Representative value for xylene; the C_8 aromatic PTR-ToF-MS signal includes xylenes and ethylbenzene. The dash indicates that a species-specific 10 s DL is not reported for the non-directly calibrated trimethylbenzene signal.

[b] Representative values for 1,2,4-trimethylbenzene; the PTR-ToF-MS signal represents unresolved trimethylbenzene isomers.

S2 Flight-specific VOC variability and toluene-to-benzene ratios

Figure S1 summarizes the variability in the seven target VOC species or groups among the 17 research flights. Table S2 provides the corresponding flight-specific toluene-to-benzene (T/B) ratios and their within-flight variability.

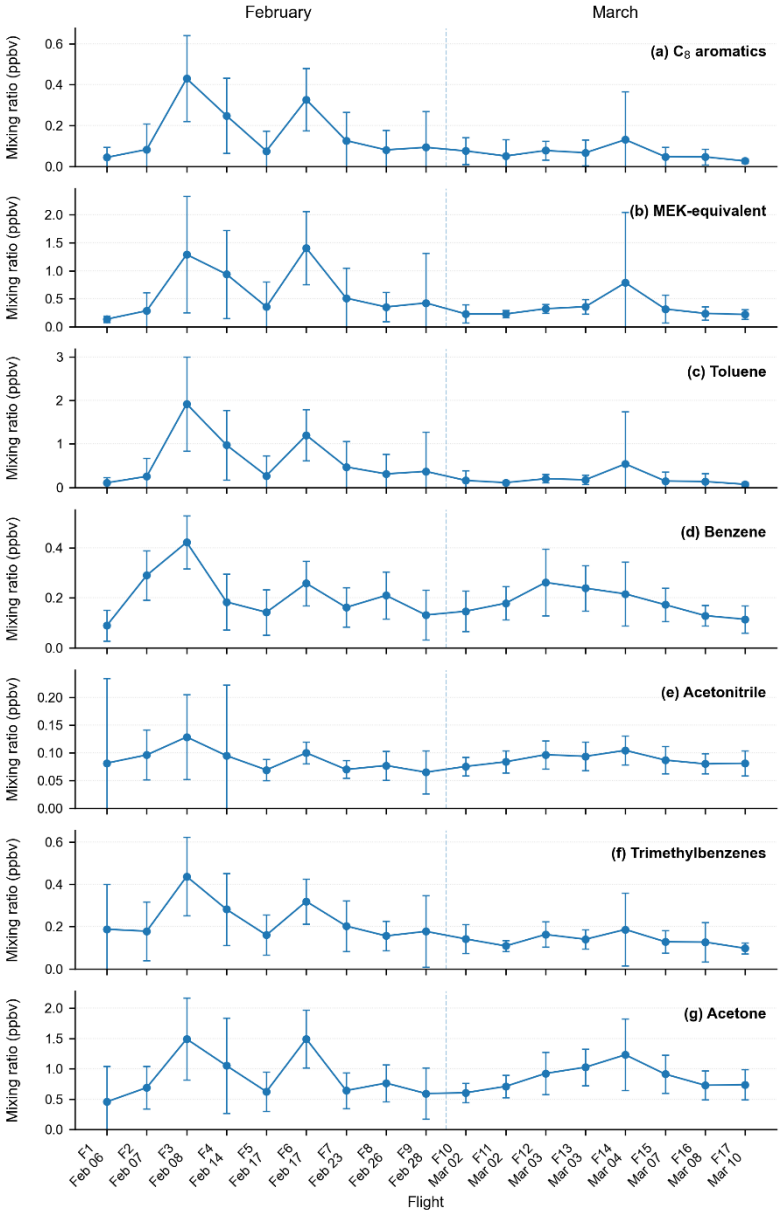


Figure S1: Variations in the seven target VOC species or groups measured aboard the Beechcraft 1900D during the ASIA-AQ campaign from 6 February to 10 March 2024, shown for each flight. Symbols represent the mean mixing ratio for each flight, and error bars indicate ±1 standard deviation.

Table S2: Flight-specific toluene-to-benzene (T/B) ratios measured aboard the Beechcraft 1900D during the ASIA-AQ campaign. Flight-mean T/B ratios were calculated as the ratio of the flight-mean toluene and benzene mixing ratios. The reported ranges represent the 10th–90th percentiles of T/B ratios calculated from the 10 s measurements within each flight. Regions are denoted as the Seoul Metropolitan Area (SMA), Yellow Sea (YS), and Gyeonggi Province (GG).

Flight	Date	Region	Flight-mean T/B	T/B (10th–90th percentile)
F1	6 Feb 2024	SMA	1.19	0.64–1.96
F2	7 Feb 2024	SMA & YS	0.87	0.40–1.53
F3	8 Feb 2024	SMA	4.55	2.02–7.42
F4	14 Feb 2024	SMA	5.30	1.26–7.49
F5	17 Feb 2024	SMA & YS	1.88	0.50–2.89
F6	17 Feb 2024	SMA	4.65	1.29–5.76
F7	23 Feb 2024	SMA & YS	2.91	0.49–6.43
F8	26 Feb 2024	SMA & YS	1.48	0.35–3.91
F9	28 Feb 2024	SMA & YS	2.80	0.84–2.87
F10	2 Mar 2024	SMA & YS	1.09	0.59–1.39
F11	2 Mar 2024	GG & YS	0.61	0.42–0.87
F12	3 Mar 2024	SMA & YS	0.76	0.54–1.21
F13	3 Mar 2024	SMA & YS	0.73	0.48–1.32
F14	4 Mar 2024	SMA & YS	2.50	0.46–4.58
F15	7 Mar 2024	GG & YS	0.85	0.42–1.37
F16	8 Mar 2024	SMA & YS	1.04	0.48–1.74
F17	10 Mar 2024	YS	0.63	0.39–0.92

S3 Additional information on NASA DC-8 observations

S3.1 DC-8 VOC measurements

The 1900D and NASA DC-8 had distinct observational roles during the South Korea component of ASIA-AQ. The DC-8, with higher flight speed, broader altitude coverage, and greater endurance, was suited for regional-scale surveys over the Yellow Sea and inland Korea. In contrast, the 1900D, with lower airspeed and repeated low-altitude sampling, resolved concentration gradients within the planetary boundary layer (PBL) over Seoul, Bucheon, and the Ansan–Sihwa industrial area. The DC-8 flight tracks and the altitude sampling distributions of both aircraft are shown in Fig. S2, with peak sampling fractions near 500 m for the 1900D and 1200 m for the DC-8.

The DC-8 deployed VOC measurement systems with different sampling characteristics. The University of Oslo provided 1 Hz VOC measurements using a FUSION Proton-Transfer-Reaction Time-of-Flight Mass Spectrometer (FUSION PTR-ToF-MS; Ionicon Analytik, Innsbruck, Austria; Reinecke et al., 2023). The Trace Organic Gas Analyzer coupled with a time-of-flight mass spectrometer (TOGA-TOF) collected discrete VOC samples for 35 s

approximately every 2 min using in situ fast online gas chromatography-mass spectrometry (GC-MS). University of California, Irvine (UCI) whole air samples (WAS) were collected in canisters on demand, with individual canister fill times ranging from 12 to 100 s (average 35 s); samples were collected every 2.6 min on average. The canister samples were subsequently analyzed in the laboratory using gas chromatography coupled with flame ionization detectors (FIDs), electron capture detectors (ECDs), and mass spectrometric detectors. Thus, PTR-ToF-MS provided high-time-resolution measurements, whereas TOGA-TOF and WAS provided discrete VOC measurements with different sampling intervals and spatial coverage (Table S3). Detailed descriptions of these measurements have been reported previously (Apel et al., 2015; Colman et al., 2001; Jeong et al., 2026; Reinecke et al., 2023; Simpson et al., 2020). The University of Oslo PTR-ToF-MS benzene data were revised after an interference affecting measurements over urban areas was identified. Accordingly, PTR-ToF-MS benzene data were not used for comparisons involving inland and urban regions; TOGA-TOF and WAS benzene measurements were used where applicable. For the chemical phase-space analysis in Fig. 8, TOGA-TOF benzene and toluene mixing ratios, originally reported in pptv, were converted to ppbv for consistency with the VOC units used throughout this study.

The two aircraft also differed substantially in their altitude sampling (Fig. S2(b)). The DC-8 sampled the Yellow Sea and inland regions over a broad altitude range and frequently represented more regionally mixed air masses. The 1900D observations were concentrated at lower altitudes, particularly within the planetary boundary layer, and repeatedly sampled source-influenced regions in and around the Seoul Metropolitan Area. Vertical profiles from the same-date observations are shown in Fig. S3.

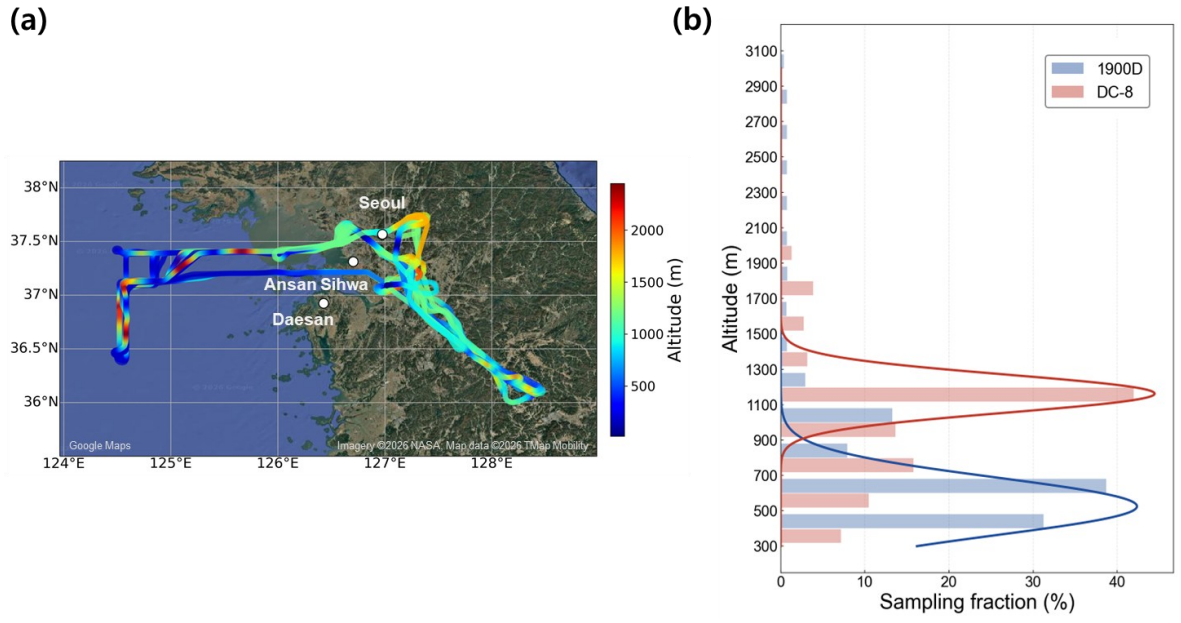


Figure S2: Flight tracks and altitude sampling of the NASA DC-8 during the South Korea component of the ASIA-AQ campaign. (a) DC-8 flight tracks, colored by aircraft altitude. White markers denote Seoul, the Ansan–Sihwa industrial complex, and the Daesan petrochemical complex. (b) Altitude sampling distributions of the 1900D PTR-ToF-MS (blue) and DC-8 TOGA-TOF (red) over the inland region (longitude ≥ 126° E) during same-date observations; bars show the fraction of measurements within 200 m altitude bins and solid curves show Gaussian fits.

Table S3: Platform and VOC instrument sampling characteristics for the NASA DC-8 and Hanseo University 1900D during the ASIA-AQ campaign. Spatial resolution was estimated using the mean true air speed (TAS) and the actual

sample duration. PTR-ToF-MS spatial resolution was calculated using a 1 s measurement interval, TOGA-TOF using its 35 s sample duration, and WAS using its 12–100 s canister fill duration. Dashes indicate instruments not deployed on the platform.

Parameter	NASA DC-8	1900D
Platform characteristics		
Mean TAS	116.5 m s^{-1} (226 kts)	83.3 m s^{-1} (162 kts)
Primary flight altitude	0.5–2 km (88 %)	0.3–1 km (76 %)
VOC instruments and temporal resolution		
PTR-ToF-MS	~1 s	~1 s
TOGA-TOF (online GC-MS)	~2 min sampling interval (35 s sample collection)	—
WAS (canister)	~2.6 min average sampling interval (12–100 s fill time; mean 35 s)	—
Spatial resolution		
PTR-ToF-MS (1 s)	~117 m	~83 m
TOGA-TOF (35 s)	~4.1 km	—
WAS (12–100 s)	~1.4–11.7 km (mean ~4.1 km)	—

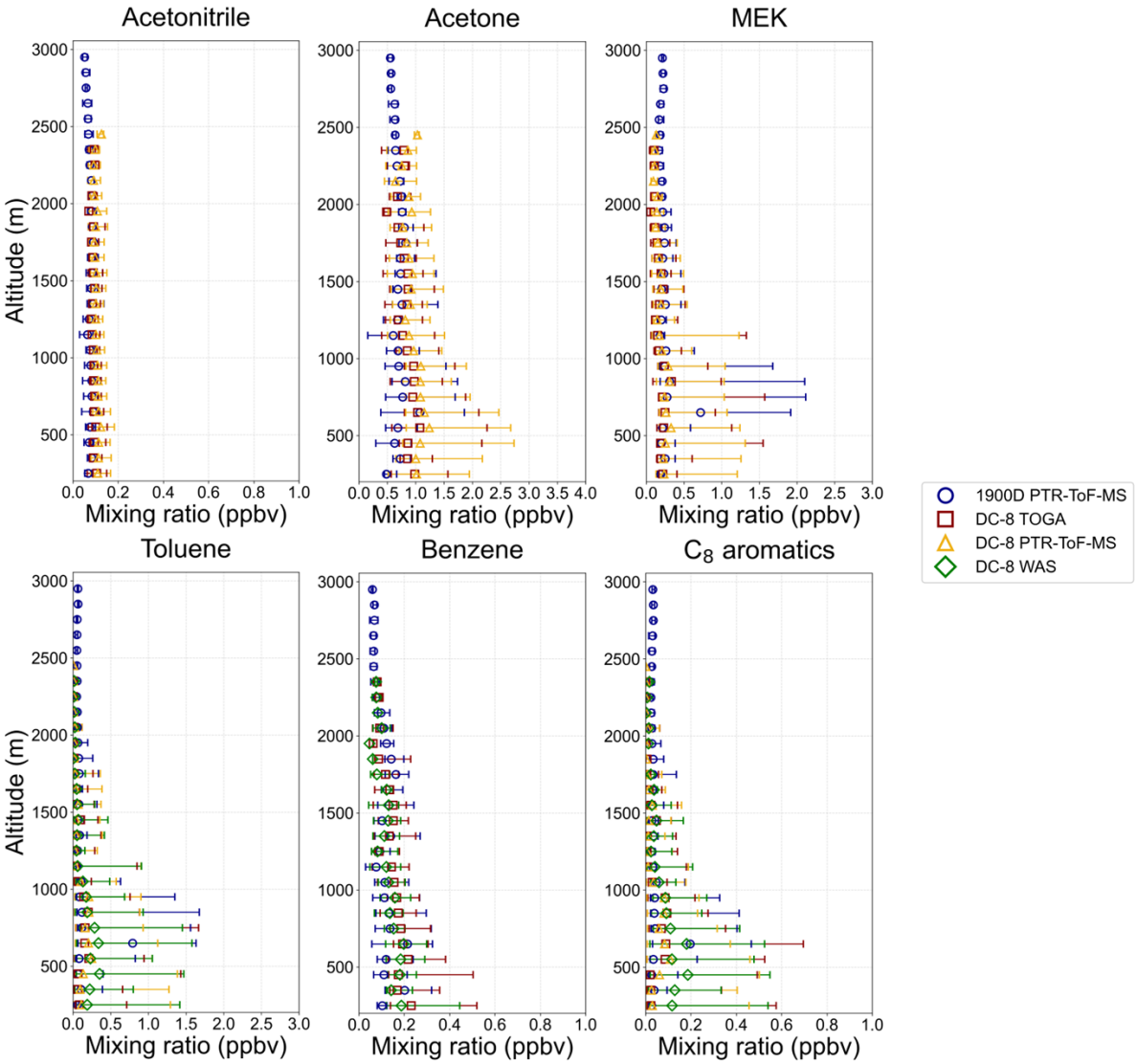


Figure S3: Vertical profiles of selected VOC mixing ratios measured by the 1900D and NASA DC-8 during same-date observations over Korea. DC-8 observations were obtained from TOGA-TOF, PTR-ToF-MS, and WAS, depending on species, while 1900D data were measured by PTR-ToF-MS. Profiles are shown for acetonitrile, acetone, MEK/MEK-equivalent signal, toluene, benzene, and C_8 aromatics. Symbols indicate median mixing ratios within each altitude bin, and error bars represent the 10th–90th percentile range.

S3.2 DC-8 trace-gas measurements

CO, CO_2, O_3, NO, and NO_2 measurements from the NASA DC-8 were used to construct the $CO/CO_2–O_3/NO_x$ chemical phase space shown in Fig. 8. CO was measured using the Differential Absorption Carbon Monoxide Measurement (DACOM) instrument, and CO_2 was measured by non-dispersive infrared spectroscopy using a modified LI-COR 7000 analyzer (Miech et al., 2025). O_3 was measured using the FastO_3 chemiluminescence instrument, and NO and NO_2 with the NSF NCAR two-channel NO/NO_2 chemiluminescence instrument. These measurements were provided at 1 Hz resolution. The CO/CO_2 ratio was calculated directly from the observed CO (ppbv) and CO_2 (ppmv) mixing ratios to examine regional differences in air mass characteristics associated with atmospheric processing and transport, as reflected in the $CO/CO_2–O_3/NO_x$ chemical phase space distributions. NO_x was calculated as the sum of NO and NO_2, with both concentrations converted from pptv to ppbv before calculation of the O_3/NO_x ratio.

S4 HYSPLIT backward-trajectory analysis

To provide transport context for representative Yellow Sea observations, 72 h backward trajectories were calculated with the Hybrid Single-Particle Lagrangian Integrated Trajectory (HYSPLIT) model (Rolph et al., 2017; Stein et al., 2015), using Global Data Assimilation System (GDAS) meteorological data. For the paired analysis, trajectories were initialized at an elevated arrival level of approximately 1950 m above ground level (AGL) and a near-surface arrival level of approximately 300 m AGL at the same sampling location. A separate low-altitude trajectory was examined for the 2 March 2024 Yellow Sea maximum case.

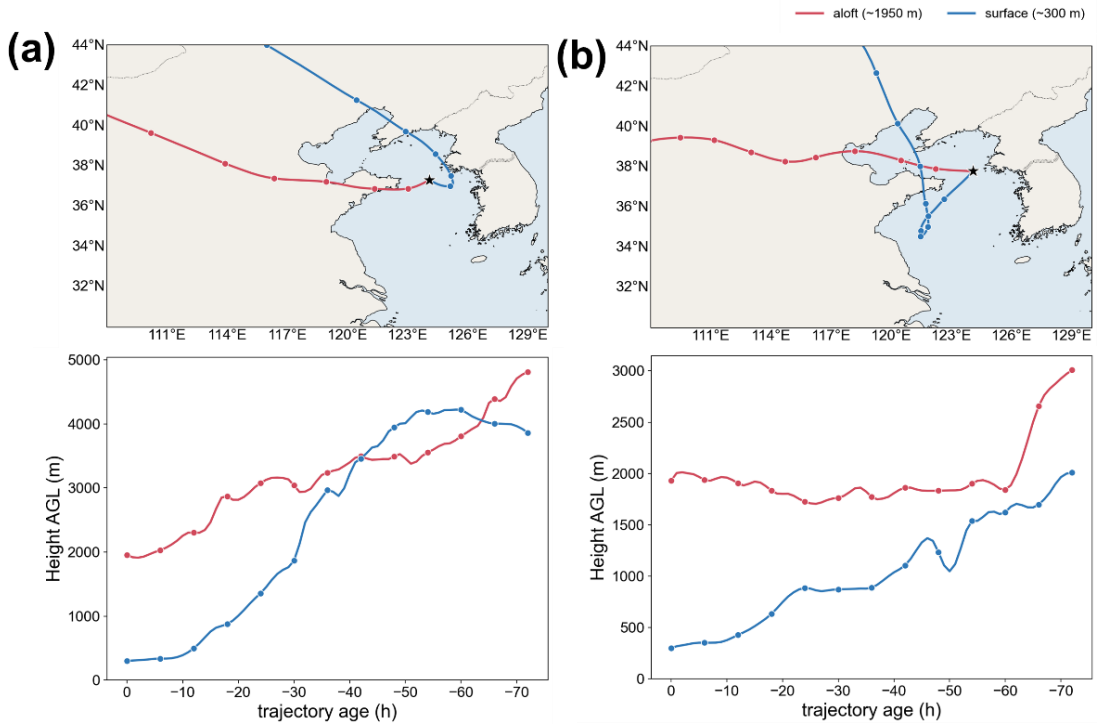


Figure S4: Paired 72 h HYSPLIT backward trajectories for two representative Yellow Sea cases. Red trajectories correspond to the aloft arrival level (~1950 m AGL), and blue trajectories correspond to the near-surface arrival level (~300 m AGL). The upper panels show horizontal transport pathways, and the lower panels show trajectory height above ground level as a function of trajectory age. Black stars mark the arrival locations.

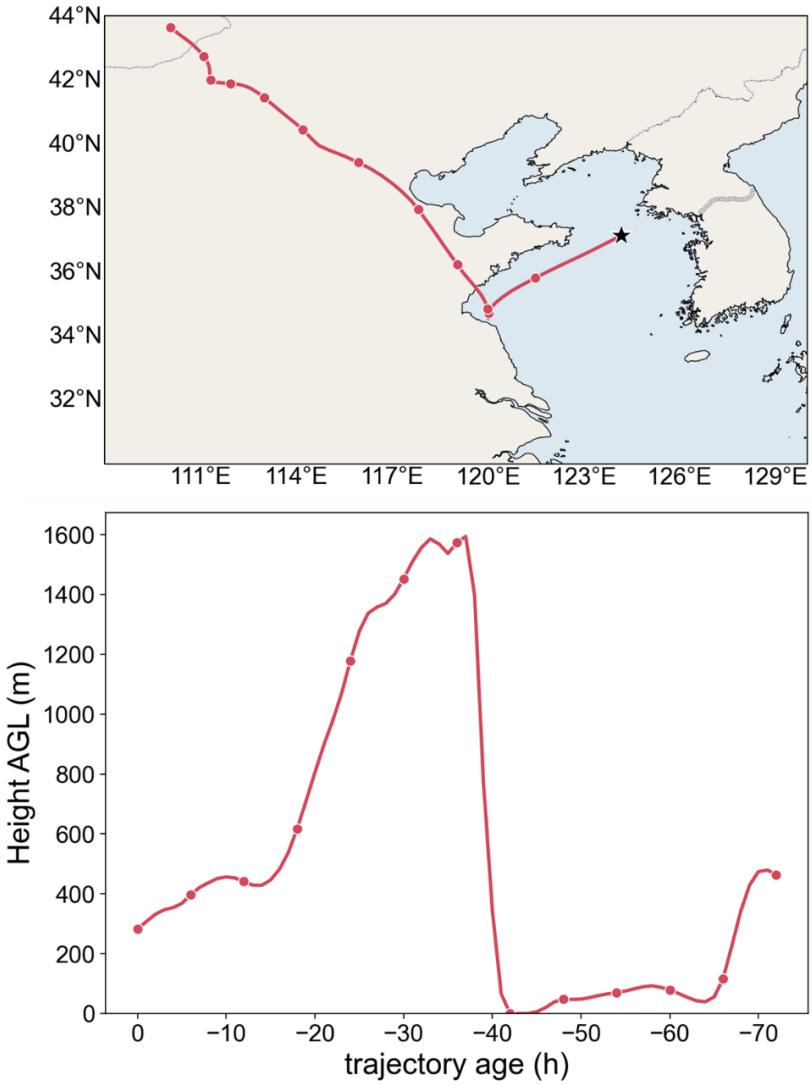


Figure S5: Seventy-two-hour HYSPLIT backward trajectory for the 2 March 2024 low-altitude Yellow Sea maximum case. The upper panel shows the horizontal transport pathway, and the lower panel shows trajectory height above ground level as a function of trajectory age. The black star marks the arrival location.

S5 OH reaction rate constants and representative lifetimes

The reactivity analysis in Fig. 5 uses representative OH-reaction lifetimes calculated from literature OH reaction rate constants (Atkinson and Arey, 2003; Le Calvé et al., 1998; Hynes and Wine, 1991), assuming a daytime OH concentration of 2.0×10^6 molecules cm^{-3} for 12 h d^{-1}. For unresolved PTR-ToF-MS signals, representative OH reaction rate constants or lifetimes were used as described in Table S4. The inverse lifetime ($1/\tau$) was used as a relative indicator of atmospheric reactivity in the analysis.

Table S4: OH reaction rate constants and representative atmospheric lifetimes used in the reactivity analysis shown in Fig. 5.

Species / signal	k_{OH} at 298 K (cm^3 $molecule^{-1}$ s^{-1})	Calculated τ_{OH} (d)	Lifetime used in Fig. 5 (d)	Basis / note
Toluene	5.63×10^{-12}	2.06	2.1	Individual compound
C_8 aromatics	1.45×10^{-11}	0.80	0.8	Representative value for unresolved ethylbenzene + xylene signal; unweighted mean of ethylbenzene and o-, m-, and p-xylene k_{OH} values
Trimethylbenzenes	—	0.30	0.3	Representative lifetime for unresolved TMB signal
1,2,3-Trimethylbenzene	3.27×10^{-11}	0.35	—	Individual TMB isomer
1,2,4-Trimethylbenzene	3.25×10^{-11}	0.36	—	Individual TMB isomer
1,3,5-Trimethylbenzene	5.67×10^{-11}	0.20	—	Individual TMB isomer
MEK-equivalent signal	1.22×10^{-12}	9.49	9.5	Representative of the MEK-equivalent signal
Acetone	1.84×10^{-13}	62.9	60	Rounded representative lifetime
Acetonitrile	2.63×10^{-14}	440	400	Rounded representative lifetime used in Fig. 5

Note: OH-reaction lifetimes (in days) were calculated as $\tau_{OH} = [k_{OH}[OH]\ (12 \times 3600\ s)]^{-1}$, using a fixed 12 h daytime-average OH concentration of 2.0×10^6 molecules cm^{-3}. Representative lifetimes were used for unresolved PTR-ToF-MS signals. For trimethylbenzenes, the representative lifetime of 0.3 d corresponds approximately to the mean of the individual OH-reaction lifetimes of 1,2,3-, 1,2,4-, and 1,3,5-trimethylbenzene (0.35, 0.36, and 0.20 d, respectively).

S6 Distance dependence used for the Yellow Sea transport scaling

The distance-based scaling applied to the 124° E eastward transport equivalent was derived from the observed offshore-to-coastal gradients of benzene and toluene. The distributions used for this empirical scaling are shown in Fig. S6.

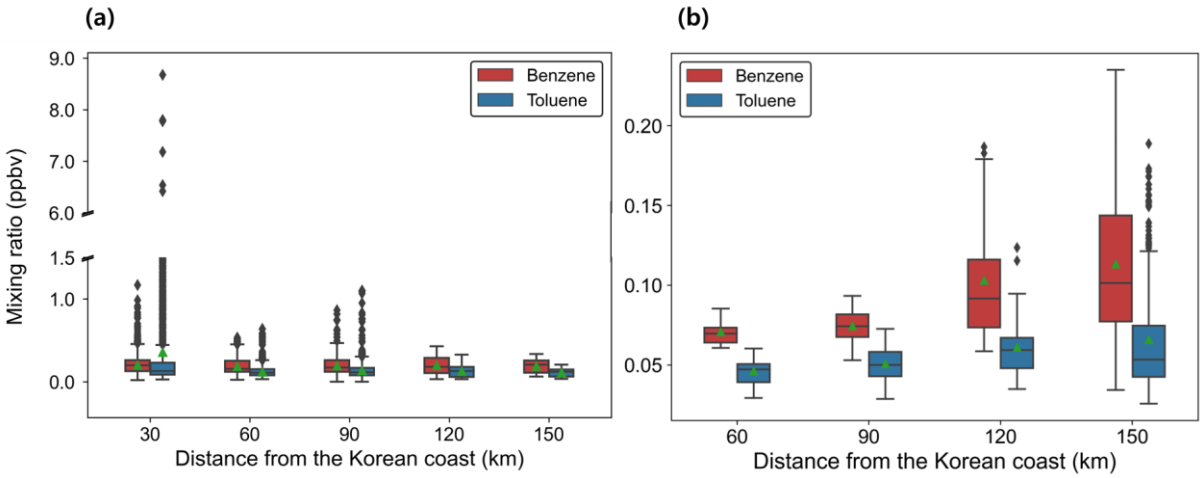


Figure S6: Distance dependence of benzene and toluene mixing ratios from the Korean coast. Boxplots show benzene and toluene mixing ratios as a function of geodesic distance from the nearest Korean coastline for observations (a) within the operational PBL (<1100 m) and (b) above the PBL (1100–3000 m). Boxes indicate the interquartile range, horizontal lines denote the median, and green triangles indicate the mean. These distributions were used to derive the empirical distance-based scaling factor applied to the 124° E eastward transport equivalent.

References

Apel, E. C., Hornbrook, R. S., Hills, A. J., Blake, N. J., Barth, M. C., Weinheimer, A., Cantrell, C., Rutledge, S. A., Basarab, B., Crawford, J., Diskin, G., Homeyer, C. R., Campos, T., Flocke, F., Fried, A., Blake, D. R., Brune, W., Pollack, I., Peischl, J., Ryerson, T., Wennberg, P. O., Crounse, J. D., Wisthaler, A., Mikoviny, T., Huey, G., Heikes, B., O'Sullivan, D., and Riemer, D. D.: Upper tropospheric ozone production from lightning NO_x-impacted convection: Smoke ingestion case study from the DC3 campaign, J. Geophys. Res.-Atmos., 120, 2505–2523, https://doi.org/10.1002/2014JD022121, 2015.

Atkinson, R. and Arey, J.: Atmospheric degradation of volatile organic compounds, Chem. Rev., 103, 4605–4638, https://doi.org/10.1021/cr0206420, 2003.

Colman, J. J., Swanson, A. L., Meinardi, S., Sive, B. C., Blake, D. R., and Rowland, F. S.: Description of the analysis of a wide range of volatile organic compounds in whole air samples collected during PEM-Tropics A and B, Anal. Chem., 73, 3723–3731, https://doi.org/10.1021/ac010027g, 2001.

Hynes, A. J. and Wine, P. H.: Kinetics and mechanism of the reaction of hydroxyl radicals with acetonitrile under atmospheric conditions, J. Phys. Chem., 95, 1232–1240, https://doi.org/10.1021/j100156a037, 1991.

Jeong, D., Hornbrook, R. S., Hills, A. J., Diskin, G., Halliday, H. S., DiGangi, J. P., Fried, A., Richter, D., Walega, J., Weibring, P., Hanisco, T. F., Wolfe, G. M., St. Clair, J., Peischl, J., Wisthaler, A., Mikoviny, T., Nowak, J. B., Piel, F., Tomsche, L., Holmes, C. D., Soja, A., Gargulinski, E., Crawford, J. H., Dibb, J., Warneke, C., Schwarz, J., and Apel, E. C.: Trace Organic Gas Analyzer Time-of-Flight mass spectrometer (TOGA-TOF) system for airborne observations of formaldehyde, Atmos. Meas. Tech., 19, 2985–3000, https://doi.org/10.5194/amt-19-2985-2026, 2026.

Le Calvé, S., Hitier, D., Le Bras, G., and Mellouki, A.: Kinetic Studies of OH Reactions with a Series of Ketones, J. Phys. Chem. A, 102, 4579–4584, https://doi.org/10.1021/jp980848y, 1998.

Miech, J. A., DiGangi, J. P., Diskin, G. S., Choi, Y., Moore, R. H., Ziemba, L. D., Gallo, F., Jordan, C. E., Shook, M. A., Wiggins, E. B., Winstead, E. L., Roy, S., Lee, Y. R., Ball, K., Crounse, J. D., Wennberg, P., Piel, F., Swift, S., Wojnowski, W., and Wisthaler, A.: Technical note: Identifying biomass burning emissions during ASIA-AQ using greenhouse gas enhancement ratios, Atmos. Chem. Phys., 25, 15701–15714, https://doi.org/10.5194/acp-25-15701-2025, 2025.

Reinecke, T., Leiminger, M., Jordan, A., Wisthaler, A., and Müller, M.: Ultrahigh sensitivity PTR-MS instrument with a well-defined ion chemistry, Anal. Chem., 95, 11879–11884, https://doi.org/10.1021/acs.analchem.3c02669, 2023.

Rolph, G., Stein, A., and Stunder, B.: Real-time Environmental Applications and Display sYstem: READY, Environ. Model. Softw., 95, 210–228, https://doi.org/10.1016/j.envsoft.2017.06.025, 2017.

Simpson, I. J., Blake, D. R., Blake, N. J., Meinardi, S., Barletta, B., Hughes, S. C., Fleming, L. T., Crawford, J. H., Diskin, G. S., Emmons, L. K., Fried, A., Guo, H., Peterson, D. A., Wisthaler, A., Woo, J. H., Barré, J., Gaubert, B., Kim, J., Kim, M. J., Kim, Y., Knote, C., Mikoviny, T., Pusede, S. E., Schroeder, J. R., Wang, Y., Wennberg, P. O., and Zeng, L.: Characterization, sources and reactivity of volatile organic compounds (VOCs) in Seoul and surrounding regions during KORUS-AQ, Elementa, 8, 37, https://doi.org/10.1525/elementa.434, 2020.

Stein, A. F., Draxler, R. R., Rolph, G. D., Stunder, B. J. B., Cohen, M. D., Ngan, F.: NOAA's HYSPLIT atmospheric transport and dispersion modeling system, b. am. meteorol. Soc., 96, 2059–2077, https://doi.org/10.1175/BAMS-D-14-00110.1, 2015.